The Role of Redox-Active Amino Acids on Compound I Stability, Substrate Oxidation, and Protein Cross-Linking in Yeast Cytochrome c Peroxidase †

4 AUTHORS, INCLUDING:

Thomas D Pfister
Leidos Biomedical Research, Inc.

37 PUBLICATIONS   **767** CITATIONS

The Role of Redox-Active Amino Acids on Compound I Stability, Substrate Oxidation, and Protein Cross-Linking in Yeast Cytochrome c Peroxidase[†]

Thomas D. Pfister,[‡] Alan J. Gengenbach,[§,||] Sung Syn,[§] and Yi Lu*,[‡,§]

Departments of Biochemistry and Chemistry, University of Illinois at Urbana−Champaign, Urbana, Illinois 61801

Received July 6, 2001; Revised Manuscript Received September 27, 2001

ABSTRACT: The role of two tryptophans (Trp51 and Trp191) and six tyrosines (Tyr36, Tyr39, Tyr42, Tyr187, Tyr229, and Tyr236) in yeast cytochrome c peroxidase (CcP) has been probed by site-directed mutagenesis. A series of sequential mutations of these redox-active amino acid residues to the corresponding, less oxidizable residues in lignin peroxidase (LiP) resulted in an increasingly more stable compound I, with rate constants for compound I decay decreasing from 57 s^{-1} for CcP(MI, W191F) to 7 s^{-1} for CcP-(MI, W191F,W51F,Y187F,Y229F,Y236F,Y36F,Y39E,Y42F). These results provide experimental support for the proposal that the stability of compound I depends on the number of endogenous oxidizable amino acids in proteins. The higher stability of compound I in the variant proteins also makes it possible to observe its visible absorption spectroscopic features more clearly. The effects of the mutations on oxidation of ferrocytochrome c and 2,6-dimethoxyphenol were also examined. Since the first mutation in the series involved the change of Trp191, a residue that plays a critical role in the electron transfer pathway between CcP and cyt c, the ability to oxidize cyt c was negligible for all mutant proteins. On the other hand, the W191F mutation had little effect on the proteins' ability to oxidize 2,6-dimethoxyphenol. Instead, the W51F mutation resulted in the largest increase in the k_{cat}/K_M, from 2.1×10^2 to 5.0×10^3 M^{-1} s^{-1}, yielding an efficiency that is comparable to that of manganese peroxidase (MnP). The effect in W51F mutation can be attributed to the residue's influence on the stability and thus reactivity of the ferryl oxygen of compound II, whose substrate oxidation is the rate-determining step in the reaction mechanism. Finally, out of all mutant proteins in this study, only the variant containing the Y36F, Y39E, and Y42F mutations was found to prevent covalent protein cross-links in the presence of excess hydrogen peroxide and in the absence of exogenous reductants. This finding marks the first time a CcP variant is incapable of forming protein cross-links and confirms that one of the three tyrosines must be involved in the protein cross-linking.

Redox-active amino acids, such as tyrosines and tryptophans, can form radicals under oxidative conditions and have been shown to play important roles in protein catalysis and cellular oxidative stress. Understanding the exact location and the nature of the protein radicals and their effect on the structure and function of proteins has been the subject of intense study (*1*). One primary example is the elucidation of the role of tyrosine and tryptophan radicals in peroxidase activity of heme proteins such as myoglobins (*2*) and peroxidases (*3−6*).

Reaction of H$_2$O$_2$ with ferric heme in myoglobins or peroxidases results in a state that is two oxidizing equivalents above the resting state (*6, 7*). One of the oxidizing equivalents

is stored as the oxyferryl [Fe(IV)=O] state. In most peroxidases, such as horseradish peroxidase (HRP),[1] lignin peroxidase (LiP), and manganese peroxidase (MnP), the other oxidizing equivalent is stored as a stable porphyrin π cation radical. The resulting heme protein is called compound I. On the other hand, in myoglobin (Mb) and cytochrome c peroxidase (CcP), the porphyrin π cation radical is observed only transiently or not at all. Instead, the second oxidizing equivalent is manifested as a stable protein radical. To differentiate this state from the compound I mentioned above, compound ES has often been used to refer to the state with

* To whom correspondence should be addressed. Tel: (217) 333-2619. Fax: (217) 333-2685. E-mail: yi-lu@uiuc.edu.
‡ Department of Biochemistry, University of Illinois at Urbana−Champaign.
§ Department of Chemistry, University of Illinois at Urbana−Champaign.
|| Current address: Department of Chemistry, Santa Clara University, 500 El Camino Real, Santa Clara, CA 95053.

[1] Abbreviations: CcP, cytochrome c peroxidase; WTCcP, wild-type CcP [in this paper, it is a recombinant CcP expressed in *Escherichia coli* with Met-Ile at the N-terminus, i.e., CcP(MI)]; CcP(WYM1), CcP-(MI) with W191F mutation; CcP(WYM2), CcP(MI) with W191F/W51F mutations; CcP(WYM3), CcP(MI) with W191F/W51F/Y187F mutations; CcP(WYM4), CcP(MI) with W191F/W51F/187F/Y229F/Y236F mutations; CcP(WYM5), CcP(MI) with W191F/W51F/Y187F/Y229F/Y236F/Y36F/Y39E/Y42F mutations; CD, circular dichroism; CT, charge transfer; cyt c, cytochrome c; 2,6-DMP, 2,6-dimethoxyphenol; EPR, electron paramagnetic resonance; HRP, horseradish peroxidase; LiP, lignin peroxidase; Mb, myoglobin; MCD, magnetic circular dichroism; MnP, manganese peroxidase; NMR, nuclear magnetic resonance; RR, resonance Raman; SDS−PAGE, sodium dodecyl sulfate−polyacrylamide gel electrophoresis; UV−vis, electronic absorption in the ultraviolet and visible region.

a stable protein radical as the second oxidizing equivalent in C*c*P (8–13).

The location of the radical and the mechanism of its formation in myoglobin have been investigated by a variety of biochemical and biophysical techniques (14–23). From the studies, both tryptophan and tyrosine radicals have been observed. For sperm whale Mb, the tryptophan radical is primarily located at Trp14 while the tyrosine radical is at either Tyr103 or Tyr151. In human Mb, an additional cysteine radical was also observed (22, 23). The studies support a model in which the second oxidizing equivalent is spread over a few redox-active amino acids, at least some of which are in equilibrium with each other (2, 20, 21). These radical formations are responsible for both the protein–protein and protein–heme cross-linking observed in the system.

While Mb contains a limited number of tryptophans and tyrosines (two tryptophans and three tyrosines for sperm whale Mb), C*c*P from *Saccharomyces cerevisiae* has an unusually high number of tryptophans (seven) and tyrosines (fourteen) for its size (34 kDa). These numbers are high even when compared with other peroxidases of similar size, such as horseradish peroxidase (one Trp and four Tyr), ascorbate peroxidase (two Trp and seven Tyr), lignin peroxidase (three Trp and no Tyr), and manganese peroxidase (one Trp and no Tyr). For years, C*c*P was one of a few proteins known to utilize a protein radical for its function, which is believed to be the oxidation of cytochrome *c* (3–6). The primary location of the protein radical in C*c*P was proposed to be either tryptophan (Trp51 or Trp191) or methionine (Met172, Met230, or Met231) on the basis of spectroscopic (8, 9, 24–26) and crystallographic (27, 28) studies. Site-directed mutagenesis of the above residues ruled out all but Trp191 as the site of the protein radical (10, 29, 30). On the other hand, the W191F mutation resulted in a dramatic decrease in C*c*P activity toward cytochrome *c* oxidation (31), as well as significant perturbation of spectroscopic signatures assigned to the protein radical (32–34). These results strongly suggested that Trp191 was either the radical site or intimately involved in the protein radical formation. Electron nuclear double resonance (ENDOR) studies with deuterated methionine or tryptophan of C*c*P variants, including the W191F mutant protein, showed that Trp191 was the primary site of the radical (11, 35, 36).

The W191F mutation in C*c*P allowed not only the identification of Trp191 as the primary site of the protein radical but also the observation of the porphyrin π cation radical for the first time (32). This occurrence may also explain the presence of Phe at the corresponding position of Trp191 in other peroxidases (such as HRP, LiP, and MnP) that display stable porphyrin π cation radicals. However, the lifetime of the porphyrin π cation radical in Trp191Phe C*c*P is quite short ($t_{1/2} \sim$14 ms) (32). EPR and ENDOR studies of the variant suggested that the porphyrin π cation radical decayed into a tyrosine-based radical (33, 34). Interestingly, in the absence of exogenous reductant, the lifetimes of the porphyrin π cation radical vary between peroxidases. For example, the half-life of the radical in HRP and MnP is about 20 and 89 min, respectively (5, 6), while the half-life in LiP is only a few seconds (37). The lifetime of the porphyrin π cation radical in peroxidases has been loosely correlated to the number of endogenous redox-active amino acids present

in the polypeptide chain (5). Therefore, it is interesting to investigate the role of tryptophans and tyrosines on the lifetime of the porphyrin π cation radical.

The EPR and ENDOR spectroscopic signals observed in the Trp191Phe mutant protein that were attributed to a tyrosine radical were also present in the compound ES of wild-type C*c*P (WTC*c*P) (9, 10, 33, 34). However, these signals in WTC*c*P were quite minor (0.05–0.2 spin) when compared with the predominant signals from the Trp191 radical ($\sim$1 spin). This observation indicates that, even though Trp191 is the primary location of the protein radical during the normal catalytic cycle of C*c*P, the radical may spread onto other redox-active amino acids, especially when no substrate (ferrocyt *c*) or other exogenous reductants are present. This observation is consistent with findings that compound ES of WTC*c*P and its W191F and W51F variants decayed spontaneously back to the resting ferric C*c*P, with concomitant destruction of redox-active amino acids such as tryptophans and tyrosines, especially when excess ($\geq$10 equiv) H_2O_2 was used (38–42). Higher molecular weight species were observed in the decay products (42–44). Peptide mapping of tryptic digests of the WTC*c*P dimer indicated a dityrosine cross-link localized between residues 32 and 48, a sequence that includes Tyr36, Tyr39, and Tyr42 (43). Furthermore, Tyr236 was proposed to be an alternate radical site to Trp191 when it was specifically modified by 2-aminothiazole in peroxide-oxidized Trp191Gly C*c*P (45). A recent multifrequency high-field EPR study dismisses Tyr236 as the alternate site and instead proposes it to be at Tyr187, Tyr244, or Tyr251 (46).

Given the importance of tryptophans and tyrosines in influencing the lifetime of compound I and providing alternate radical sites for catalysis and for protein cross-linking, we have made a series of site-directed mutants of C*c*P, where two of the tryptophans in the active site and six tyrosines on the proximal side (including Tyr36, Tyr39, Tyr42, and Tyr236) have been replaced with the corresponding residues of LiP. The effects of the sequential removal of these endogenous redox-active amino acids on the lifetime of compound I, substrate oxidation, and protein cross-linking are reported.

EXPERIMENTAL PROCEDURES

Materials. HPLC-purified oligonucleotide primers (50 nmol scale) were ordered from Operon Technologies (Alameda, CA). Native and cloned *Pfu* polymerases were purchased from Stratagen (San Diego, CA). Restriction enzymes and T4 DNA ligase were purchased from Gibco (Gaithersburg, MD) or New England Biolabs (Beverly, MA) except *Dpn*I, which is obtained from Stratagen. XL-1 Blue and BL-21 *Escherichia coli* cell strains were from Novagen (Madison, WI) and were stored as frozen glycerol stocks. NaCl, 30% hydrogen peroxide, Difco bacto-tryptone, and yeast extract were purchased from Fisher Scientific (Pittsburgh, PA). Horse heart cytochrome *c* was obtained from Sigma (St. Louis, MO). Plasmid DNA purification kits were purchased from Qiagen (Valencia, CA). Protein chromatography columns and chromatography materials were obtained from Pharmacia (Piscataway, NJ). YM-10 membranes, stirred-cell ultrafiltration apparatus, and Centricon-10 were from Amicon (Beverly, MA). The low-range prestained SDS–PAGE

Table 1: Summary of Variant Proteins under Investigation

name	mutation	Soret shift pK_a	$\epsilon_{408}{}^a$ (mM^{-1} cm^{-1})	MW (Da) calcd	MW (Da) obsd
WTCcP	CcP(MI)		113	33730.6	33731.0 ± 2.8
CcP(WYM1)	CcP(MI, W191F)		115	33691.2	33690.9 ± 2.0
CcP(WYM2)	CcP(MI, W191F, W51F)	7.9	123	33652.5	33653.7 ± 2.4
CcP(WYM3)	CcP(MI, W191F,W51F,Y187F)	7.6	132	33636.6	33635.4 ± 4.2
CcP(WYM4)	CcP(MI, W191F,W51F,Y187F,Y229F,Y236F)	7.3	126	33608.0	33608.2 ± 2.8
CcP(WYM5)	CcP(MI, W191F,W51F,Y187F,Y229F,Y236F,Y36F,Y39E,Y42F)	6.5	131	33538.0	33537.5 ± 2.6

^{a} At pH 6.0.

protein standards were from Bio-Rad Laboratories (Hercules, CA). Polymerase chain reactions and QCM reactions were performed using a PTC-100 thermal cycler from MJ Research (Watertown, MA). DNA sequencing was performed by the University of Illinois Biotechnology Center, and the University of Illinois Mass Spectroscopy facility performed mass spectral analysis. Unless otherwise noted, chemicals were obtained from commercial sources and used without further purification. A hydrogen peroxide stock solution was stored in the absence of light and the concentration determined by titration against KMnO$_4$ or by UV absorption at 240 nm (*47*).

Construction, Expression, and Purification of Site-Directed Mutant Proteins. Construction, expression, and purification of site-directed mutant proteins were performed as described previously (*48−50*). The CcP(MI) gene containing the Met-Ile codon at the beginning was used as the template for site-directed mutagenesis (*30*). The expressed protein with Met-Ile at the N-terminus is identical to the native CcP in structural and functional properties (*30*) and is thus called wild-type CcP (WTCcP) in this paper. The primers for each mutation were designed so that mutations caused insertion or deletion of restriction sites in the plasmid containing the CcP gene. The successful mutation was first screened by restriction digests and then confirmed by DNA sequencing and mass spectrometry of the purified proteins (results shown in Table 1). Protein concentrations were calculated using the extinction coefficients (ϵ_{408}) shown in Table 1, determined by a hemochromagen assay (*51*, *52*). The extinction coefficients were the average of at least two trials.

Electronic Absorption (UV−Vis) and Circular Dichroism (CD) Studies. UV−vis spectra were obtained using a Hewlett-Packard 8453 spectrophotometer. The samples were in 50 mM potassium phosphate buffer at pH values specified in the text or figure legends. CD spectra were taken using a Jasco 720 spectrophotometer. The enzyme stock of 100 μM was diluted to 5 μM in 50 mM phosphate, pH 6.0. The CD spectra were measured from 250 to 200 nm using a quartz cuvette with 0.1 cm path length. A scan rate of 50 nm/min was used, and spectra were the average of four scans. The observed ellipticity θ (millidegrees) was converted to molar ellipticity [θ] by dividing θ with [10(Cl)], where C is concentration (M) and l is the path length (0.1 cm) (*53*). Percent helicity (f_H) was calculated from the ellipticity at 222 nm [$f_H = -([\theta]_{222} + 2340)/30300$].

Stopped-Flow Kinetics of Compound I Formation and Decay. Stopped-flow UV−vis spectra were collected using an Applied Photophysics Ltd. (Leatherhead, U.K.) SX18.MV stopped-flow spectrometer equipped with a 256 element photodiode array detector. Reactions were carried out at 21 °C using a circulating water bath. The protein and hydrogen

peroxide samples were prepared from concentrated stock solution and dissolved in 50 mM potassium phosphate, pH 6.0. The hydrogen peroxide was always in excess of the proteins to maintain the pseudo-first-order conditions. Spectra were collected on a logarithmic basis for the first 10 s after mixing. Kinetic constants were obtained using a global analysis routine from the program Pro-Kineticist (Applied Photophysics Ltd.).

Ferrocytochrome c Oxidation Assay. Horse heart cytochrome *c* was reduced with dithionite. Excess dithionite was removed by passing the sample down a size exclusion (PD10) column. The concentration of ferrocytochrome *c* was determined at 550 nm using $\epsilon = 27.7$ mM^{-1} cm^{-1} (*54*). Ferrocytochrome *c* oxidation was carried out in 50 mM potassium phosphate, pH 6.0 at 25.0 °C, by monitoring absorption changes at 550 nm using a HP 8453 spectrophotometer. Initial oxidation rates were calculated using $\Delta\epsilon_{550}$ of 19.5 mM^{-1} cm^{-1} (*55*). Rates were corrected for the uncatalyzed oxidation by H$_2$O$_2$. The kinetic constants k_{cat} and K_M were obtained from the double reciprocal plot of initial rate versus substrate. The initial rates (v/e) of ferrocytochrome *c* oxidation for all variants were calculated at 10, 20, and 40 μM cyt *c* and compared to WTCcP.

2,6-DMP Oxidation Assay and Kinetics. Steady-state 2,6-DMP oxidations were performed in 50 mM phosphate, pH 6.0. For pH dependence studies, the ionic strength was adjusted by addition of KCl (data not shown). Oxidation of 2,6-DMP was monitored by formation of correglione (ϵ_{468} = 56.6 mM^{-1} cm^{-1}) from two molecules of 2,6-DMP using an HP 8453 spectrophotometer. Typical assay solutions contained 10 μL of 10 μM stock enzyme. The reactions were initiated by addition of hydrogen peroxide to a final concentration of 83.3 μM. Plots of initial rate versus substrate concentration were constructed. The slope of the linear portion of the initial rate versus substrate concentration is equal to catalytic efficiency (k_{cat}/K_M) (*56*). The k_{cat}/K_M values obtained in this manner were used to determine the 2,6-DMP activity of WTCcP and its variants.

Protein Cross-Link Analysis. Protein cross-link experiments for the WTCcP and its variants were carried out as previously described (*42*, *43*). Reactions were initiated by the addition of 10 equiv of H$_2$O$_2$ to 50 μM protein in 50 mM potassium phosphate, pH 4.5. After incubation for 30 min and 24 h, the reaction mixtures were analyzed using SDS−PAGE (*42*, *43*).

RESULTS

Site-Directed Mutation of Tryptophans and Tyrosines. Two tryptophans and six tyrosines in CcP were changed sequentially to the corresponding, less oxidizable residues in LiP
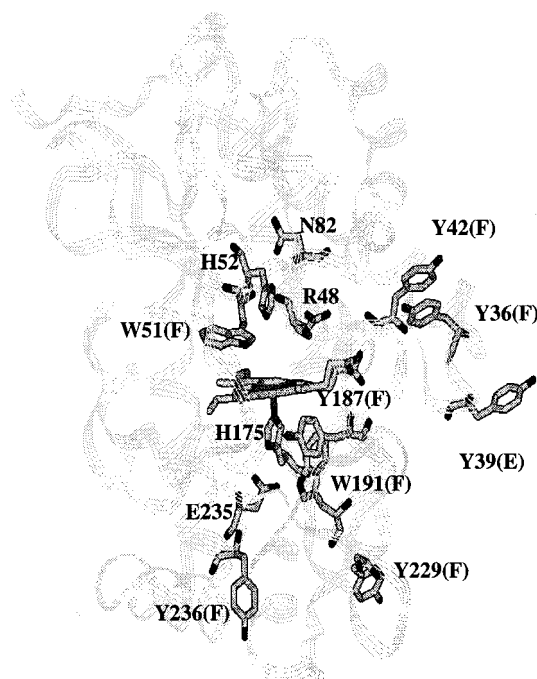
FIGURE 1: The tryptophans and tyrosines in cytochrome *c* peroxidase investigated in this study. They were mutated to corresponding residues in lignin peroxidase (shown in parentheses). Other active site residues important for the function of C*c*P are also displayed in the figure.

(see Figure 1). The C*c*P mutant proteins were constructed, expressed, and purified to homogeneity using protocols described previously (*48−50*). Table 1 lists the specific mutations, extinction coefficients, and mass spectrometric properties of the five variant proteins in this investigation. To aid the presentation and discussion of results, each mutant protein is also given a short name (see Table 1).

UV−Vis Spectroscopy. The UV−vis spectra of C*c*P-(WYM1) and C*c*P(WYM4) at pH 6.0 and 7.5 are shown in Figure 2. As reported previously (*32, 45*), C*c*P(WYM1) displays a Soret band at 408 nm and α and β bands at 540 and 505 nm, respectively (Figure 2A). A shoulder at 380 nm and an absorption band at 642 nm, assignable to a δ band and a charge-transfer (CT) band, respectively, are also present. The ratio of A_{408nm}/A_{380nm} is ∼1.7. These spectra are very similar to that of WTC*c*P and have been shown to be due to mainly a five-coordinated high-spin ferric heme (*3, 49, 50, 57−63*). This spectrum is largely unchanged from pH 4.5 to pH 7.5 (Figure 2C). At pH above 7.5, the Soret band at 408 nm decreases (Figure 2C) with concomitant absorption changes in other regions that are indicative of an alkaline transition. These behaviors are quite similar to that of WTC*c*P (*3, 49, 50, 57−63*).

C*c*P(WYM4), on the other hand, displays a spectrum with a CT band blue shifted from 642 to 637 nm and a higher A_{408nm}/A_{380nm} ratio at 2.7 at pH 6.0. The spectrum is typical of a six-coordinated high-spin ferric heme. However, at pH 7.5, the Soret, α, and β bands shift to 414, 568, and 536 nm, respectively. The characteristic high-spin ferric heme charge transfer band is also absent at this pH, indicating that, at high pH, the mutant proteins contain low-spin ferric heme. The pK_a of this transition is determined from the pH titration curve (Figure 2C) and is listed in Table 2. At pH above 8.5, the Soret band decreases even further, and the spectral change
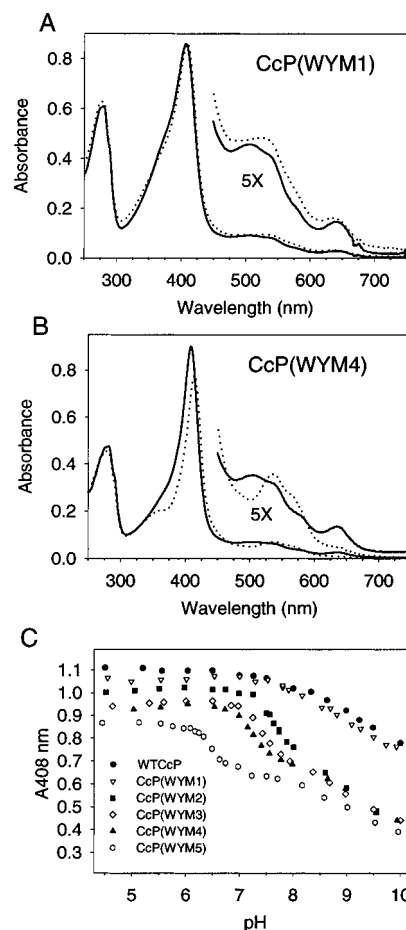

FIGURE 2: UV−vis spectra of (A) C*c*P(WYM1) and (B) C*c*P-(WYM4) in 50 mM potassium phosphate, pH 6.0 (solid line) and pH 7.5 (dotted line). (C) pH-dependent absorbance changes of the Soret band at 408 nm. For clarity, data points in pH curves have been offset.

Table 2: Rate Constants ($k_{2,obs}$) for the Decay of Compound I to Compound II and Catalytic Efficiencies (k_{cat}/K_M) of 2,6-DMP Oxidation by C*c*P and Variants

	$k_{2,obs}$ (s^{-1})	k_{cat}/K_M (M^{-1} s^{-1}) × 10^2
C*c*P(MI)		2.1
C*c*P(WYM1)	57	1.2
C*c*P(WYM2)	17	50
C*c*P(WYM3)	14	50
C*c*P(WYM4)	8	51
C*c*P(WYM5)	7	56
MnP[77]		95
rMnP[78]		40
rMnP S168W[78]		3000
rLiP[78]		4700

is indicative of an alkaline transition as seen in C*c*P(WYM1) and WTC*c*P (Figure 2C). The UV−vis spectra and their pH-dependent behavior of C*c*P(WYM2), C*c*P(WYM3), and C*c*P-(WYM5) are very similar to those of C*c*P(WYM4) (data not shown). Their pH titration curves are shown in Figure 2C. The pK_a's of pH-dependent spectral transitions for C*c*P-(WYM3−5) are summarized in Table 2.

Circular Dichroism (CD) Spectroscopy. The CD spectra in the UV region of WTC*c*P and all variants listed in Table 1 are shown in Figure 3. The spectra all show a maximum at 210 nm and a broad shoulder around 222 nm. The spectra are all consistent with α-helical secondary structure, with
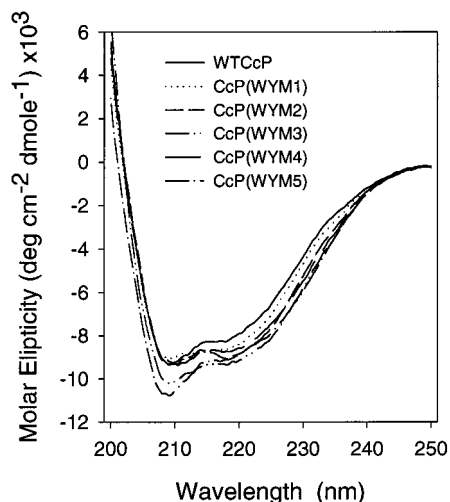
FIGURE 3: Circular dichroim (CD) spectra of WTC*c*P and C*c*P-(WYM1−5). The proteins were in 50 mM potassium phosphate, pH 6.0.
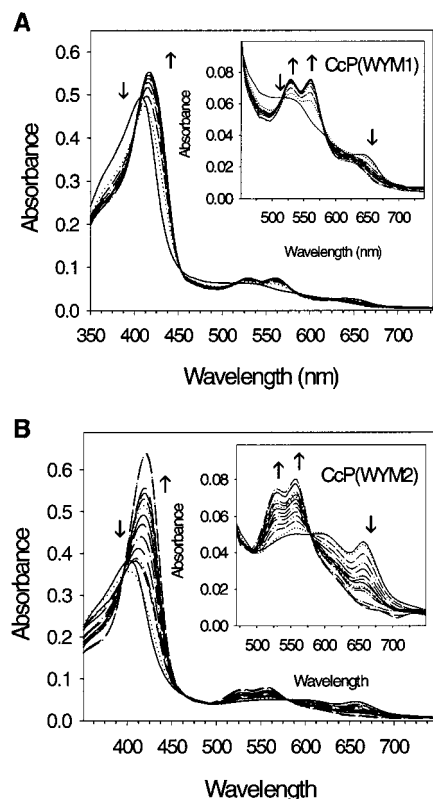

FIGURE 4: Selected stopped-flow UV−vis spectra for the reaction of (A) C*c*P(WYM1) and (B) C*c*P(WYM2) with H_2O_2 in 100 mM potassium phosphate, pH 6.0.

calculated percent α-helicity of 17% for WTC*c*P, 18% for C*c*P(WYM1), 20% for C*c*P(WYM2), 21% for C*c*P(WYM3), 19% for C*c*P(WYM4), and 20% for C*c*P(WYM5). The similarity of the observed CD spectra and calculated percent α-helicity between the variant proteins and WTC*c*P suggest that the mutations caused no major secondary structural changes.

Stopped-Flow Kinetics of Compound I Formation and Decay. The reactions of C*c*P variants with hydrogen peroxide were monitored using stopped-flow UV−vis spectroscopy. Reaction of 100 μM H_2O_2 with 5 μM C*c*P(WYM1) [C*c*P-(MI, W191F)] resulted in an immediate intensity reduction
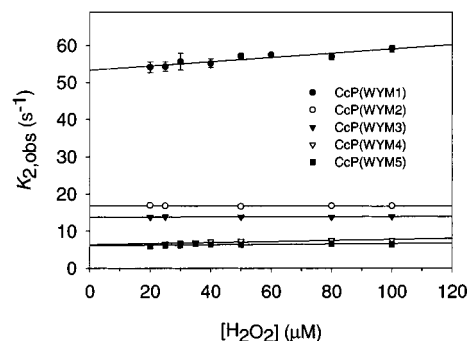

FIGURE 5: Rates of spontaneous decay of compound I to compound II ($k_{2,obs}$) in 50 mM potassium phosphate, pH 6.0. Each data point was the average of at least three trials. Where error bars are not visible, they are contained within the symbol.

of the Soret band at 408 nm (Figure 4A). The Soret band reached to the lowest intensity at ∼9 ms, after which its intensity increases with concurrent shifts of the position to 418 nm. In the visible region (Figure 4A, inset), broad absorption bands with peaks around 540, 600, and 650 nm appeared 4 ms after the reaction. The 650 nm band then decayed and shifted to ∼630 nm. At the same time, the broad absorption bands around 540 and 600 nm converted to 529 and 561 nm. The spectral changes are similar to those reported for the same mutant protein by Erman et al. (*32*). The authors attributed the spectral changes to the formation of compound I, which then decays to compound II. The final spectrum at the end of the stopped-flow study with absorptions at ∼418, 529, 561, and 630 nm matches exactly that of compound II. The strongest evidence for the formation of compound I is the dramatic reduction of the Soret band. However, the features of compound I in the visible region are not as well defined. On the other hand, reaction of 100 μM H_2O_2 with 5 μM C*c*P(WYM2) [C*c*P(MI, W191F/W51F)] resulted in much more pronounced spectral features with absorptions at ∼550, 600, and 660 nm (Figure 4B, inset). The spectrum is almost identical to that of compound I in other peroxidases such as horseradish peroxidase and lignin peroxidase (*6*). The spectral changes of C*c*P(WYM3), C*c*P-(WYM4), and C*c*P(WYM5) are qualitatively similar to those of C*c*P(WYM2) (data not shown).

The spectra were fit to the following model:

$$A \xrightarrow{k_{1,obs}} B$$
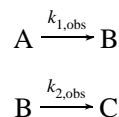
$$B \xrightarrow{k_{2,obs}} C$$

The rapid reaction precluded a rigorous determination of the pseudo-first-order rate constant ($k_{1,obs}$) for the formation of compound I. On the other hand, a rate constant for decay of compound I ($k_{2,obs}$) can be obtained. The plot of $k_{2,obs}$ vs hydrogen peroxide concentration is shown in Figure 5. Table 2 summarizes the kinetic constants obtained from the spectroscopic fits.

Ferrocytochrome c Oxidation. Kinetic constants for ferrocytochrome *c* oxidation by WTC*c*P were obtained from a double reciprocal plot of initial rate versus substrate concentration (data not shown). WTC*c*P had a k_{cat} of 420 s^{-1} and K_M of 3.1 μM. Initial rates of the variants were compared to WTC*c*P at three different substrate concentrations. The rates for C*c*P(WYM1−5) at 10, 20, and 40 μM cyt *c*, shown

Table 3: Cytochrome *c* Oxidation by CcP(MI) and Variants[a]

[cyt *c*] (μM)	CcP(MI)	CcP(WYM1)	CcP(WYM2)	CcP(WYM3)	CcP(WYM4)	CcP(WYM5)
10	100 (335)	0.08	0.03	0.05	0.06	0.04
20	100 (371)	0.08	0.05	0.07	0.07	0.03
40	100 (437)	0.06	0.05	0.08	0.08	0.10

[a] Rates are relative to CcP(MI) at given concentrations of cyt *c*. v/e (s^{-1}) of CcP(MI) is in parentheses.
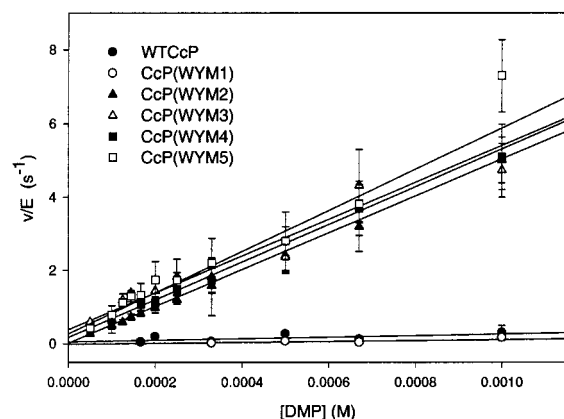

FIGURE 6: 2,6-DMP oxidation catalyzed by WTCcP and CcP-(WYM1−5). Oxidation reactions were carried out in 50 mM potassium phosphate, pH 6.0 at 25 °C. Each data point is the average of at least three trials. Where error bars are not visible, they are contained within the symbol.

in Table 3, ranged from 0.03% to 0.1% of the respective WTCcP rates at the given cyt *c* concentration.

Oxidation of 2,6-DMP. The H_2O_2-dependent oxidation of 2,6-DMP by WTCcP and CcP(WYM1−5) was carried out in 50 mM phosphate, pH 6.0 at 25 °C. No oxidation was observed in the absence of enzyme or H_2O_2 (data not shown). The plot of initial rates with respect to the substrate concentration is shown in Figure 6. All plots are essentially linear over the entire range. From the plot, the k_{cat}/K_M of the reaction for WTCcP and all variants was obtained and is summarized in Table 2.

Protein Cross-Link Study. The extent of protein cross-links upon reaction of excess H_2O_2 with ferric enzyme was analyzed by SDS−PAGE. As shown in Figure 7, incubation of purified WTCcP monomer (lane 2) with 10 equiv of H_2O_2 for 30 min resulted in a substantial decrease in intensity of the monomer band (lane 3), with the appearance of bands with molecular weights corresponding to a CcP dimer. Other less clear bands also appear at higher molecular weights, likely corresponding to trimers, tetramers, and other multimers. CcP(WYM1−4) showed almost identical results (lanes 4−11). In contrast, the CcP(WYM5) monomer (lane 12) showed no significant decrease in intensity and little evidence for dimer or other multimer formation (lane 13). Incubation of CcP(WYM5) with 10 equiv of H_2O_2 for 24 h produced an almost identical result.

DISCUSSION

Probing the Role of Tryptophans and Tyrosines in CcP through Site-Directed Mutagenesis. With seven tryptophans and fourteen tyrosines, CcP contains an unusually high number of redox-active amino acid residues for its 34 kDa size. To investigate the role of the tryptophans and tyrosines in the structure and function of heme enzymes, we chose a
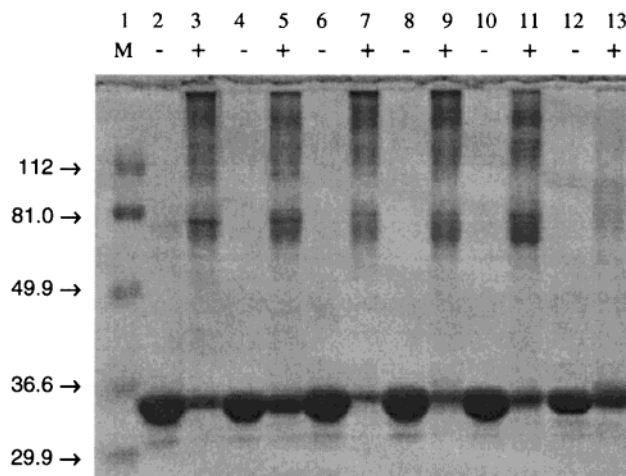

FIGURE 7: SDS−PAGE analysis of protein cross-linking in WTCcP and CcP(WYM1−5). Incubations of the proteins with and without 10 equiv of H_2O_2 were carried out as described in Experimental Procedures. Lanes: 1, protein molecular weight markers; 2, WTCcP without H_2O_2; 3, WTCcP with H_2O_2; 4, CcP(WYM1) without H_2O_2; 5, CcP(WYM1) with H_2O_2; 6, CcP(WYM2) without H_2O_2; 7, CcP-(WYM2) with H_2O_2; 8, CcP(WYM3) without H_2O_2; 9, CcP-(WYM3) with H_2O_2; 10, WYCcPM4 without H_2O_2; 11, CcP-(WYM4) with H_2O_2; 12, CcP(WYM5) without H_2O_2; 13, CcP-(WYM5) with H_2O_2.

subset of these residues, focusing on those that are close to the heme and whose roles have been implicated in previous studies. Both Trp191 on the proximal side and Trp51 on the distal side (Figure 1) have been investigated extensively by site-directed mutagenesis (*11*, *12*, *29−36*, *42*, *45*, *50*, *59*, *60*, *64*, *65*). Almost all of the published work focused on individual tryptophans. We wish to extend the work to include a variant protein containing the W191F/W51F double mutation and compare its properties with those of individual mutations. Another unique aspect of this work is a systematic probe of the role of several tyrosines in CcP including (a) Tyr187, which is close to the heme and Trp191 and has been proposed to be a potential alternate radical site (*46*), (b) Tyr229, which is close to the primary Trp191 radical site and may play a role in funneling the primary radical, (c) Tyr236, which has been proposed to be an alternate radical site to Trp191 because reaction between 2-aminothiazole and peroxide-oxidized W191G resulted in the specific covalent modification at this site (*45*), and (d) Tyr36, Tyr39, and Tyr42, which were implicated to be potential sites of protein−protein cross-linking when CcP is reacted with excess H_2O_2 in the absence of exogenous reductants (*43*).

Our strategy to probe the role of the above tryptophans and tyrosines is to change them into other, less oxidizable, residues by site-directed mutagenesis. To minimize structural perturbation from the mutations, we changed the tryptophans and tyrosines into corresponding residues in LiP, a peroxidase that shares a similar overall structure with CcP and contains no observable protein radicals (*66*, *67*). To aid in the

presentation and discussion of the results, we name these variant proteins with sequential mutations as CcP(WYM1) (with W191F mutation), CcP(WYM2) (with W191F/W51F mutations), CcP(WYM3) (with W191F/W51F/Y187F mutations), CcP(WYM4) (with W191F/W51F/187F/Y229F/Y236F mutations), and CcP(WYM5) (with W191F/W51F/Y187F/Y229F/Y236F/Y36F/Y39E/Y42F mutations). The definition of the names and their properties are summarized in Table 1.

UV−Vis and CD Spectroscopic Characterization. WTCcP is known to contain a five-coordinated high-spin heme with a low A_{408}/A_{380} ratio (at 1.51) and a charge-transfer band above 640 nm (at ∼645 nm) (*3, 62, 63, 68*). In addition, it maintains the same five-coordinated high-spin form between pH 5.5 and pH 7.5. At pH 7.5, alkaline transition occurs, resulting in further intensity reduction at the Soret band (Figure 2C). The spectra and their pH-dependent behavior of CcP(WYM1) (Figure 2A,C) are quite similar to those of WTCcP. In contrast, with the exception of the alkaline transitions at pH above 7.5, CcP(WYM2−5) variants are different from CcP(WYM1) and WTCcP. At pH below 6.0, CcP(WYM2−5) variants display UV−vis spectral characteristics of a six-coordinated high-spin heme. The spectrum of CcP(WYM4) is shown in Figure 2B as an example. It is characterized by the high A_{Soret}/A_{380} ratio (at 2.7) and a charge transfer band below 640 nm (at ∼637 nm). At pH above 7.5, however, the UV−vis spectra of the variant proteins clearly indicate that the proteins are in the low-spin heme form. The major difference between the CcP(WYM2−5) variants is the pK_a at which the transition from the high-spin state to the low-spin state occurs (Table 2); the pK_a decreases from 7.9 for CcP(WYM2) to 6.5 for CcP(WYM5), indicating that introducing more mutations into CcP resulted in increasingly lower pK_a for the spin state transition.

Six-coordinated high-spin species and the pH-dependent spin state changes have been observed in other CcP variants, and the assignment of the state has been supported by other spectroscopic studies such as EPR, MCD, RR, and NMR (*3, 49, 50, 57−63*). The X-ray crystal structure of WTCcP showed that there are three well-defined water molecules in the distal side of heme pocket (*27, 69*). They are held away from the heme iron by a hydrogen-bonding network. It is generally believed that mutations in both sides of heme can result in the disruption of the hydrogen-bonding network and thus make it easy for the water molecule to bind to the heme iron to form six-coordinated high-spin heme at low pH and for the heme to be converted to low spin at high pH (*3, 49, 50, 57−63*). The low-spin heme at pH above 7.5 often inhibited ligand binding and reaction (data not shown). Therefore, all of the stopped-flow kinetic studies and substrate oxidation studies were carried out using freshly prepared proteins in phosphate buffer at pH 6.0, where all variants remain in the high-spin heme form.

Despite these different pH-dependent behaviors, the CD spectra of the variant proteins are quite similar to that of WTCcP (Figure 3), suggesting that the mutations caused no major changes in the overall secondary structure. The mutations of these redox-active residues are expected to exert many interesting effects on the function of the proteins. In this report, we wish to focus on their effects on the lifetime of compound I, on oxidation of cytochrome *c* and 2,6-dimethoxyphenol, and on protein−protein cross-linking.

Effects of Mutations on Compound I Formation and Its Stability. The stability of compound I varies greatly among the various heme peroxidases. Although the formation of compound I is believed to precede compound ES formation in CcP, compound I in WTCcP has not been observed. As first observed by Erman et al. in a stopped-flow UV−vis study (*32*), reaction of H_2O_2 with CcP(MI, W191F) [corresponding to CcP(WYM1) in this study; see Table 1] resulted in transient formation of compound I. Compound I then decayed to compound ES containing a ferryl species and a protein radical (Figure 4A). Similar conclusions can be obtained from the spectral changes of reaction of H_2O_2 with other variant proteins in Table 1 (see Figure 4B). As in CcP-(MI, W191F) (*32*), the $k_{2,obs}$'s of all variant proteins in this study are independent of H_2O_2 concentration under pseudo-first-order reaction conditions (Figure 5). This result is expected since the decay of compound I to compound II involves only internal radical transfer from the porphyrin to an amino acid, without participation of exogenous H_2O_2.

There are, however, two major differences among the variant proteins. First, the rates of compound I decay, $k_{2,obs}$, decrease from 57 s^{-1} for CcP(WYM1) to 7 s^{-1} for CcP-(WYM5) (Table 2). These results suggest strongly that compound I stability increases when more tryptophans and tyrosines are converted to less oxidizable phenylalanines and glutamate. The effects on the lifetime of compound I appear to be cumulative. Our results provide experimental support for the proposal that the stability of compound I depends on the number of endogenous oxidizable amino acids in proteins (*5*). Furthermore, our results also indicate that the effect is *not* additive; the biggest drop in compound I decay rate occurred when the W191F and W51F mutations were introduced.

The differences in compound I stability of different variants also affected the ability to observe distinct spectroscopic features of compound I. In CcP(WYM1), where compound I is the least stable among the variants, the absorption spectrum in the visible region resembles that of compound I at the earliest time point (4 ms) of the stopped-flow experiment (Figure 4A, inset). However, the spectrum was not well defined and was rapidly converted to that of compound II. On the other hand, the higher stability of compound I in CcP(WYM2) made it possible to observe the characteristic visible spectrum of compound I (at ∼550, 600, and 660 nm) as well as its well-defined transition to compound II (Figure 4B, inset). These results provide stronger support for the presence of compound I in CcP lacking redox-active amino acids and for the involvement of these amino acids as alternate sites of protein radicals.

Effect of Mutations on Ferrocytochrome c Oxidation and 2,6-DMP Oxidation. Since ferrocytochrome *c* oxidation is a common activity assay for CcP, we investigated the effects of Trp and Tyr mutations on the CcP activity. The parameters we obtained for WTCcP (k_{cat} of 420 s^{-1} and K_M of 3.1 μM) are in agreement with previously reported values (*3*). In contrast, the variant proteins in this study possessed only 0.03−0.10% of the activity of WTCcP (Table 3). These results are not surprising because all variant proteins investigated here contain the W191F mutation. Trp191 has been shown to be the primary location of the protein radical (*11, 35, 36*) and is critical in the electron transfer pathway between CcP and cyt *c* (*70*). Proteins containing the W191F

mutation have been shown to possess negligible activity toward ferrocytochrome *c* oxidation (*31*). The low activity that is detected could arise from cyt *c* binding at a second, low-affinity, binding site, which has been identified (*71*–*74*). Interestingly, previous studies of the Trp51Phe C*c*P single mutant protein showed that the mutation resulted in a higher turnover rate toward cyt *c* oxidation, with apparent k_{cat} up to 6 times greater than that of WTC*c*P (*29*, *30*, *59*). However, the data presented here indicated that the same W51F mutation cannot rescue any of the loss of cyt *c* oxidation activity in Trp191Phe/Trp51Phe double mutant protein. This result provides another strong evidence for the dominant role played by the Trp191 in cyt *c* oxidation.

Since the tryptophans and tyrosines were changed to the corresponding residues in LiP, we also investigated the effects of the mutations on 2,6-DMP oxidation, a common assay for fungal peroxidases, such as MnP and LiP (*6*, *66*, *75*). While the catalytic efficiency of C*c*P(WYM1) containing the W191F mutation is slightly less than that of WTC*c*P, the efficiency of C*c*P(WYM2) containing the W191F/W51F mutations showed a significant (∼24-fold) increase in efficiency over that of WTC*c*P (Table 2). These results indicated that, even though both W191F and W51F mutations helped to stabilize compound I, only the W51F mutation has a major effect on 2,6-DMP oxidation.

Trp51 lies in the distal side of the heme pocket, with its indole ring oriented parallel to the heme plane (Figure 1). Significantly, the indole ring nitrogen forms a hydrogen bond with one of the crystallographically well-defined water molecules in the pocket and within hydrogen-bonding distance to the ferryl oxygen of compound I or II. Mutations of Trp51 to other residues including Phe have resulted in C*c*P variants that are more active toward cyt *c* oxidation and the oxidation of small organic molecules such as aniline derivatives (*12*). Furthermore, while mutation of Trp191 to Phe in MnC*c*P, a C*c*P variant with an engineered Mn(II) binding site at a location similar to that in MnP, also led to a slight decrease in catalytic efficiency for manganese oxidation, the W191F/W51F double mutation in MnC*c*P showed a 6-fold increase (*50*, *76*). The effect of W51F mutation was attributed to its ability to disrupt the hydrogen bond to the ferryl oxygen, decreasing the stability of the ferryl oxygen of compound II, and in turn increase the reactivity of compound II, whose substrate oxidation is the rate-determining step in the reaction mechanism (*12*, *50*, *59*, *76*). Similar conclusions can be drawn from the current study. The fact that C*c*P(WYM3–5) variants did not show any further increase in the catalytic efficiency is consistent with the above conclusion because the C*c*P(WYM3–5) variants all contain the W51F mutation and all other mutations in the variants are far away from the ferryl oxygen of compound II and thus exert little influence on the reactivity of compound II.

Interestingly, the catalytic efficiency of C*c*P(WYM2–5) for 2,6-DMP oxidation is similar to that observed for MnP from *P. ostreatus* (*77*) and rMnP from *P. chrysosporium* (*78*) (Table 2). However, the efficiency is still 83–93-fold lower than rLiP from *P. chrysosporium* (*78*). The difference is likely attributable to the presence of Trp171 on the surface of LiP (*67*, *79*–*81*). Trp171 forms a transient radical that has been shown to be vital to the catalytic mechanism of veratryl alcohol oxidation by LiP (*82*, *83*). In addition, the

Cβ position of Trp171 is hydroxylated in an autocatalytic manner during turnover; its function, however, is still under investigation (*80*, *81*, *84*, *85*). Mutation of Trp171 (W171F and W171S) resulted in a nearly complete loss of veratryl alcohol oxidation activity, while retaining 2,2′-azinobis(3-ethylbenzothiazoline-6-sulfonic acid) oxidation activity, suggesting the existence of two separate substrate interaction sites (*82*). The introduction of a Trp in rMnP (S164W) at the homologous position of rLiP Trp171 resulted in a dramatic increase of catalytic efficiency for 2,6-DMP oxidation, from over 100-fold less to within only 1.6-fold that of rLiP (*78*). It is therefore feasible to render similar increases in 2,6-DMP oxidation efficiency by engineering a Trp in C*c*P(WYM2–5) at the homologous position to W171 in LiP.

Effect of Mutations on Protein Cross-Linking. As discussed in the introduction, several early studies have shown that reaction of C*c*P or its variants with excess H_2O_2 in the absence of exogenous reductants resulted in loss of redox-active amino acids such as tryptophans and tyrosines (*38*–*42*). The loss of amino acids was quantified by both amino acid analysis and protein steady-state fluorescence spectroscopy. Furthermore, the reaction also resulted in protein–protein cross-links through tyrosine residues such as Y36, Y39, Y42 (*43*), or Y236 (*45*). By changing these and other tyrosines to phenylalanines or glutamates in a sequential manner, we have found for the first time that the protein cross-link was not observable in a variant protein [C*c*P-(WYM5)] containing Y36F/Y39E/Y42F mutations (Figure 7, lane 13) under conditions that WTC*c*P and all other variant proteins were cross-linked. These results provide a strong support that Y36, Y39, or Y42 are involved in the linkage. It is unlikely that changes in the protein structure are due to the loss of cross-linking activity since C*c*P(WYM5) retains the ability to react with H_2O_2 and the CD spectrum is very similar to that of WTC*c*P.

In summary, a new series of C*c*P variants with redox-active tryptophans and tyrosines changed to less easily oxidized amino acids were constructed, expressed, purified, and characterized. Sequential mutation of W191F, W51F, Y187F, Y229F, Y236F, Y36F, Y39E, and Y42F resulted in accumulative higher stability of compound I. While the W191F mutation resulted in the largest decrease in cyt *c* oxidation activity, the W51F mutation caused the largest increase in oxidation of 2,6-DMP. Finally, this variant series was used to confirm that one of Tyr36, Tyr39, or Tyr42 is involved in protein cross-linking in the presence of excess H_2O_2. Mutation of individual Tyr residues may provide more conclusive evidence. Further biophysical studies using EPR and fluorescence spectroscopy of these variants are underway to provide more information about the nature and location of the alternate protein radical(s).

REFERENCES

1. Stubbe, J., and van der Donk, W. A. (1998) *Chem. Rev. 98*, 705–762.
2. Raven, E. L., and Mauk, A. G. (2001) *Adv. Inorg. Chem. 51*, 1–49.

Pfister et al.

3. Bosshard, H. R., Anni, H., and Yonetani, T. (1991) in *Peroxidases in Chemistry and Biology* (Grisham, J. E. M. B., Ed.) pp 51−84, CRC Press, Boca Raton, FL.

4. Poulos, T. L., and Fenna, R. E. (1994) in *Metalloenzymes Involving Amino Acid-Residue and Related Radicals, Vol. 30 of Metal Ions in Biological Systems* (Sigel, H., and Sigel, A., Eds.) pp 25−75, Marcel Dekker, New York.

5. English, A. M., and Tsaprailis, G. (1995) *Adv. Inorg. Chem. 43*, 79−125.

6. Dunford, H. B. (1999) *Heme Peroxidases*, Wiley-VCH, New York.

7. Dawson, J. H. (1988) *Science 240*, 433−439.

8. Yonetani, T., and Schleyer, H. (1966) *J. Biol. Chem. 241*, 3240−3243.

9. Hori, H., and Yonetani, T. (1985) *J. Biol. Chem. 260*, 349−355.

10. Goodin, D. B., Mauk, A. G., and Smith, M. (1986) *Proc. Natl. Acad. Sci. U.S.A. 83*, 1295−1299.

11. Sivaraja, M., Goodin, D. B., Smith, M., and Hoffman, B. M. (1989) *Science 245*, 738−740.

12. Roe, J. A., and Goodin, D. B. (1993) *J. Biol. Chem. 268*, 20037−20045.

13. Pond, A. E., Bruce, G. S., English, A. M., Sono, M., and Dawson, J. H. (1998) *Inorg. Chim. Acta 275−276*, 250−255.

14. Tew, D., and Ortiz de Montellano, P. R. (1988) *J. Biol. Chem. 263*, 17880−17886.

15. Catalano, C. E., Choe, Y. S., and Ortiz de Montellano, P. R. (1989) *J. Biol. Chem. 264*, 10534−10541.

16. Wilks, A., and Ortiz de Montellano, P. R. (1992) *J. Biol. Chem. 267*, 8827−8833.

17. Fenwick, C. W., and English, A. M. (1996) *J. Am. Chem. Soc. 118*, 12236−12237.

18. Gunther, M. R., Kelman, D. J., Corbett, J. T., and Mason, R. P. (1995) *J. Biol. Chem. 270*, 16075−16081.

19. DeGray, J. A., Gunther, M. R., Tschirret-Guth, R., Ortiz de Montellano, P. R., and Mason, R. P. (1997) *J. Biol. Chem. 272*, 2359−2362.

20. Gunther, M. R., Tschirret-Guth, R. A., Witkowska, H. E., Fann, Y. C., Barr, D. P., De Montellano, P. R. O., and Mason, R. P. (1998) *Biochem. J. 330*, 1293−1299.

21. Irwin, J. A., Ostdal, H., and Davies, M. J. (1999) *Arch. Biochem. Biophys. 362*, 94−104.

22. Witting, P. K., Douglas, D. J., and Mauk, A. G. (2000) *J. Biol. Chem. 275*, 20391−20398.

23. Witting, P. K., and Mauk, A. G. (2001) *J. Biol. Chem. 276*, 16540−16547.

24. Hoffman, B. M., Roberts, J. E., Brown, T. G., Kang, C. H., and Margoliash, E. (1979) *Proc. Natl. Acad. Sci. U.S.A. 76*, 6132−6136.

25. Hoffman, B. M., Roberts, J. E., Kang, C. H., and Margoliash, E. (1981) *J. Biol. Chem. 256*, 6556−6564.

26. Lerch, K., Mims, W. B., and Peisach, J. (1981) *J. Biol. Chem. 256*, 10088−10091.

27. Finzel, B. C., Poulos, T. L., and Kraut, J. (1984) *J. Biol. Chem. 259*, 13027−13036.

28. Edwards, S. L., Xuong, N., Hamlin, R. C., and Kraut, J. (1987) *Biochemistry 26*, 1503−1511.

29. Goodin, D. B., Mauk, A. G., and Smith, M. (1987) *J. Biol. Chem. 262*, 7719−7724.

30. Fishel, L. A., Villafranca, J. E., Mauro, J. M., and Kraut, J. (1987) *Biochemistry 26*, 351−360.

31. Mauro, J. M., Fishel, L. A., Hazzard, J. T., Meyer, T. E., Tollin, G., Cusanovich, M. A., and Kraut, J. (1988) *Biochemistry 27*, 6243−6256.

32. Erman, J. E., Vitello, L. B., Mauro, J. M., and Kraut, J. (1989) *Biochemistry 28*, 7992−7995.

33. Scholes, C. P., Liu, Y., Fishel, L. A., Farnum, M. F., Mauro, J. M., and Kraut, J. (1989) *Isr. J. Chem. 29*, 85−92.

34. Fishel, L. A., Farnum, M. F., Mauro, J. M., Miller, M. A., Kraut, J., Liu, Y., Tan, X. L., and Scholes, C. P. (1991) *Biochemistry 30*, 1986−1996.

35. Houseman, A. L. P., Doan, P. E., Goodin, D. B., and Hoffman, B. M. (1993) *Biochemistry 32*, 4430−4443.

36. Huyett, J. E., Doan, P. E., Gurbiel, R., Houseman, A. L. P., Sivaraja, M., Goodin, D. B., and Hoffman, B. M. (1995) *J. Am. Chem. Soc. 117*, 9033−9041.

37. Kishi, K., Hildebrand, D. P., Kusters-van Someren, M., Gettemy, J., Mauk, A. G., and Gold, M. H. (1997) *Biochemistry 36*, 4268−4277.

38. Coulson, A. F. W., and Yonetani, T. (1972) *Biochem. Biophys. Res. Commun. 49*, 391.

39. Erman, J. E., and Yonetani, T. (1975) *Biochim. Biophys. Acta 393*, 343−349.

40. Erman, J. E., and Yonetani, T. (1975) *Biochim. Biophys. Acta 393*, 350−357.

41. Fox, T., Tsaprailis, G., and English, A. M. (1994) *Biochemistry 33*, 186−191.

42. Tsaprailis, G., and English, A. M. (1996) *Can. J. Chem. 74*, 2250−2257.

43. Spangler, B. D., and Erman, J. E. (1986) *Biochim. Biophys. Acta 872*, 155−157.

44. Miller, M. A., Vitello, L., and Erman, J. E. (1995) *Biochemistry 34*, 12048−12058.

45. Musah, R. A., and Goodin, D. B. (1997) *Biochemistry 36*, 11665−11674.

46. Ivancich, A., Dorlet, P., Goodin, D. B., and Un, S. (2001) *J. Am. Chem. Soc. 123*, 5050−5058.

47. Nelson, D. P., and Kiesow, L. A. (1972) *Anal. Biochem. 49*, 474−478.

48. Yeung, B. K., Wang, X., Sigman, J. A., Petillo, P. A., and Lu, Y. (1997) *Chem. Biol. 4*, 215−221.

49. Wang, X., and Lu, Y. (1999) *Biochemistry 38*, 9146−9157.

50. Gengenbach, A., Syn, S., Wang, X., and Lu, Y. (1999) *Biochemistry 38*, 11425−11432.

51. De Duve, C. (1948) *Acta Chem. Scand. 2*, 264−289.

52. Morrison, M., and Horie, S. (1965) *Anal. Biochem. 12*, 77−82.

53. Sievers, G. (1978) *Biochim. Biophys. Acta 536*, 212−225.

54. Margoliash, E., and Frohwirt, N. (1959) *Biochem. J. 71*, 570−572.

55. Kang, D. S., and Erman, J. E. (1982) *J. Biol. Chem. 257*, 12775−12779.

56. Casella, L., Monzani, E., Gullotti, M., Santelli, E., and Beringhelli, T. (1996) *Gazz. Chim. Ital. 126*, 121−125.

57. Smulevich, G., Mauro, J. M., Fishel, L. A., English, A. M., Kraut, J., and Spiro, T. G. (1988) *Biochemistry 27*, 5477−5485.

58. Smulevich, G., Miller, M. A., Kraut, J., and Spiro, T. G. (1991) *Biochemistry 30*, 9546−9558.

59. Goodin, D. B., Davidson, M. G., Roe, J. A., Mauk, A. G., and Smith, M. (1991) *Biochemistry 30*, 4953−4962.

60. Turano, P., Ferrer, J. C., Cheesman, M. R., Thomson, A. J., Banci, L., Bertini, I., and Mauk, A. G. (1995) *Biochemistry 34*, 13895−13905.

61. Wilcox, S. K., Putnam, C. D., Sastry, M., Blankenship, J., Chazin, W. J., McRee, D. E., and Goodin, D. B. (1998) *Biochemistry 37*, 16853−16862.

62. Pond, A. E., Sono, M., Elenkova, E. A., McRee, D. E., Goodin, D. B., English, A. M., and Dawson, J. H. (1999) *J. Inorg. Biochem. 76*, 165−174.

63. Pond, A. E., Sono, M., Elenkova, E. A., Goodin, D. B., English, A. M., and Dawson, J. H. (1999) *Biospectroscopy 5*, S42−S52.

64. Miller, V. P., DePillis, G. D., Ferrer, J. C., Mauk, A. G., and Ortiz de Montellano, P. R. (1992) *J. Biol. Chem. 267*, 8936−8942.

65. Fitzgerald, M. M., Churchill, M. J., McRee, D. E., and Goodin, D. B. (1994) *Biochemistry 33*, 3807−3818.

66. Gold, M. H., Wariishi, H., and Valli, K. (1989) *ACS Symp. Ser. 389*, 127−140.

67. Poulos, T. L., Edwards, S. L., Wariishi, H., and Gold, M. H. (1993) *J. Biol. Chem. 268*, 4429−4440.

68. Vitello, L. B., Huang, M., and Erman, J. E. (1990) *Biochemistry 29*, 4283−4288.

69. Wang, J., Mauro, J. M., Edwards, S. L., Oatley, S. J., Fishel, L. A., Ashford, V. A., Nguyen Huu, X., and Kraut, J. (1990) *Biochemistry 29*, 7160−7173.

70. Pelletier, H., and Kraut, J. (1992) *Science 258*, 1748−1755.

71. Erman, J. E., Kang, D. S., Kim, K. L., Summers, F. E., Matthis, A. L., and Vitello, L. B. (1991) *Mol. Cryst. Liq. Cryst. 194*, 253−258.

72. Matthis, A. L., and Erman, J. E. (1995) *Biochemistry 34*, 9985−9990.

73. Mei, H., Wang, K., McKee, S., Wang, X., Pielak, G. J., Durham, B., and Millett, F. (1996) *Biochemistry 35*, 15800−15806.

74. Leesch, V. W., Bujons, J., Mauk, A. G., and Hoffman, B. M. (2000) *Biochemistry 39*, 10132−10139.

75. Cai, D., and Tien, M. (1993) *J. Biotechnol. 30*, 79−90.

76. Gengenbach, A., Wang, X., and Lu, Y. (2001) in *Fundamentals and Catalysis of Oxidative Delignification Processes* (Argyropoulos, D. S., Ed.) pp 487−500, American Chemical Society, Washington, DC.

77. Sarkar, S., Martinez, A. T., and Martinez, M. J. (1997) *Biochim. Biophys. Acta 1339*, 23−30.

78. Timofeevski, S. L., Nie, G., Reading, N. S., and Aust, S. D. (2000) *Arch. Biochem. Biophys. 373*, 147−153.

79. Piontek, K., Glumoff, T., and Winterhalter, K. (1993) *FEBS Lett. 315*, 119−124.

80. Choinowski, T., Blodig, W., Winterhalter, K. H., and Piontek, K. (1999) *J. Mol. Biol. 286*, 809−827.

81. Blodig, W., Smith, A. T., Doyle, W. A., and Piontek, K. (2001) *J. Mol. Biol. 305*, 851−861.

82. Doyle, W. A., Blodig, W., Veitch, N. C., Piontek, K., and Smith, A. T. (1998) *Biochemistry 37*, 15097−15105.

83. Blodig, W., Smith, A. T., Winterhalter, K., and Piontek, K. (1999) *Arch. Biochem. Biophys. 370*, 86−92.

84. Blodig, W., Doyle, W. A., Smith, A. T., Winterhalter, K., Choinowski, T., and Piontek, K. (1998) *Biochemistry 37*, 8832−8838.

85. Piontek, K., Smith, A. T., and Blodig, W. (2001) *Biochem. Soc. Trans. 29*, 111−116.